Human Molecular Genetics, 2011, Vol. 20, No. 6 ***1154–1163***
doi:10.1093/hmg/ddq559
Advance Access published on January 3, 2011

Over-expression of BCL2 rescues muscle weakness in a mouse model of oculopharyngeal muscular dystrophy

Janet E. Davies and David C. Rubinsztein*

Department of Medical Genetics, University of Cambridge, Cambridge Institute for Medical Research, Addenbrooke's Hospital, Hills Road, Cambridge, CB2 0XY, UK

Received November 24, 2010; Revised and Accepted December 24, 2010

Oculopharyngeal muscular dystrophy (OPMD) is a late-onset muscular dystrophy caused by a polyalanine expansion mutation in the coding region of the poly-(A) binding protein nuclear 1 (*PABPN1*) gene. In unaffected individuals, $(GCG)_6$ encodes the first 6 alanines in a homopolymeric stretch of 10 alanines. In most patients, this $(GCG)_6$ repeat is expanded to $(GCG)_{8-13}$, leading to a stretch of 12–17 alanines in mutant PABPN1, which is thought to confer a toxic gain of function. Thus, OPMD has been modelled by expressing mutant *PABPN1* transgenes in the presence of endogenous copies of the gene in cells and mice. In these models, increased apoptosis is seen, but it is unclear whether this process mediates OPMD. The role of apoptosis in the pathogenesis of different muscular dystrophies is unclear. Blocking apoptosis ameliorates muscle disease in some mouse models of muscular dystrophy such as laminin α-2-deficient mice, but not in others such as dystrophin-deficient (mdx) mice. Here we demonstrate that apoptosis is not only involved in the pathology of OPMD but also is a major contributor to the muscle weakness and dysfunction in this disease. Genetically blocking apoptosis by over-expressing BCL2 ameliorates muscle weakness in our mouse model of OPMD (A17 mice). The effect of BCL2 co-expression on muscle weakness is transient, since muscle weakness is apparent in mice expressing both A17 and BCL2 transgenes at late time points. Thus, while apoptosis is a major pathway that causes muscle weakness in OPMD, other cell death pathways may also contribute to the disease when apoptosis is inhibited.

INTRODUCTION

Oculopharyngeal muscular dystrophy (OPMD) is a late-onset, progressive muscular dystrophy that typically presents with the symptoms of ptosis and dysphagia (1,2) and can proceed to affect all voluntary muscles, leading to proximal muscle weakness (3,4) and a severely impaired quality of life. OPMD is generally inherited as an autosomal dominant trait, but recessive forms do rarely occur (5). The mutation that causes OPMD was identified in 1998 and is an abnormal expansion of a $(GCG)_n$ trinucleotide repeat in the coding region of the poly-(A) binding protein nuclear 1 (*PABPN1*) gene (6). In unaffected individuals, $(GCG)_6$ codes for the first 6 alanines in a homopolymeric stretch of 10 alanines. In most patients, this $(GCG)_6$ repeat is expanded to $(GCG)_{8-13}$, leading to a stretch of 12–17 alanines in mutant PABPN1. PABPN1 with an expanded polyalanine tract forms aggregates consisting of tubular filaments within the nuclei of skeletal muscle fibres (6–8). OPMD is thought to be caused by a toxic gain of function of the polyalanine expansion mutation. Thus, the cell (9–11), mouse (12,13) and *Drosophila* (14) models of OPMD have been generated by expressing mutant *PABPN1* transgenes in the presence of endogenous copies of the gene.

We have developed a mouse model of OPMD by expressing a mutant *PABPN1* transgene (with a 17 alanine repeat, the longest OPMD-causing expansion; A17 mice) under control of the human skeletal actin promoter to drive muscle-specific expression (12). A17 mice appear normal at birth, but develop a progressive muscle weakness that is accompanied by the

*To whom correspondence should be addressed. Tel: +44 1223762608; Fax: +44 1223331206; Email: dcr1000@hermes.cam.ac.uk

formation of mutant PABPN1-containing aggregates in the nuclei of skeletal myocytes. This phenotype is not seen in mice expressing a wild-type *PABPN1* transgene (with 10 alanine repeat; A10) at similar levels (12). A17 mice have elevated levels of apoptosis, as shown by increased TUNEL-positive nuclei, active caspase 3 immuno-positive myofibres and myofibres with a cytosolic distribution of cytochrome c (15). TUNEL-positive myocyte nuclei were also seen in an alternative transgenic mouse model of OPMD in which a *PABPN1* transgene is expressed highly in all tissues under the control of the CAG (cytomegalovirus enhancer and chicken β-actin) promoter (13). Doxycycline (12), trehalose (16) and cystamine (15) alleviate muscle weakness in A17 mice. These drugs decrease A17 toxicity not only by reducing the aggregation of A17, but also appear to have distinct anti-apoptotic effects. Additional evidence suggesting a role for apoptosis in OPMD comes from cell and *Drosophila* models. Pathology in a *Drosophila* model of OPMD can be ameliorated by expression of the viral anti-apoptotic protein p35 (14). In addition, apoptotic markers are elevated in COS-7 and C2C12 cells transiently expressing mutant PABPN1, and toxicity is reduced by expression of the viral BCL2 homolog E1B19K (12).

Despite the presence of increased apoptosis in OPMD models, it is unclear whether apoptosis is an important contributor to the myofibre loss and muscle weakness in this disease. The role of apoptosis in muscle degeneration is not fully understood. While apoptosis is thought to have a central role in the pathology of some muscular dystrophies (17–27), its role in others is unclear (17,28). It is also unclear how multinucleated cells such as myofibres co-ordinate cell death signals and die. To directly assess the contribution of apoptosis to OPMD and test the relevance of apoptosis *in vivo*, we have crossbred A17 mice with mice that over-express BCL2 (B-cell CLL/lymphoma 2). *BCL2* was initially identified as a gene that is deregulated in follicular B-cell lymphomas due to t(14;18) chromosomal translocations (29), and belongs to a large family of pro- and anti-apoptotic proteins. The balance and interactions between different BCL2-family proteins control the mitochondrial apoptotic pathway and determines whether a cell lives or dies. Pro-apoptotic BAX (BCL2-associated X protein) and BAK (BCL2 homologous antagonist/killer) induce cell death by increasing the permeability of the mitochondrial membrane, causing the release of cytochrome c, which leads to the activation of downstream caspases (30). BCL2 antagonizes BAX/BAK activation and mice over-expressing BCL2 have decreased apoptosis (17). Here we demonstrate that BCL2 not only modifies the phenotype of OPMD model mice, but also regulates a central pathway of myofibre death in OPMD. *BCL2* expression reduces levels of apoptosis and markedly improves the strength of A17 muscle at early time points.

RESULTS

BCL2 expression rescues muscle weakness in A17 mice

To genetically test the role of apoptosis in the pathogenesis of OPMD, we introduced a *BCL2* transgene into A17 mice. Mice heterozgous for the A17 transgene [A17-1 mice (12)] were crossed with mice heterozygous for a muscle-expressing BCL2 transgene (17). These MRF4-hBCL2 mice express a human *BCL2* transgene at high levels in skeletal muscle under control of the myogenin regulatory 4 promoter (17). All experiments were carried out on F1 mice derived from crossing A17 mice on an FvB background with MRF4-hBCL2 mice on a C57BL/6 background. Litters comprised F1 mice expressing either A17 or BCL2 alone, non-transgenic mice and mice expressing both A17 and *BCL2* transgenes (A17 × BCL2 mice) (Fig. 1A). All mice were tested monthly up to the age of 10 months. This allowed the observation of the effects of BCL2 over-expression on early-stage muscle weakness and late-stage locomotor defects that are part of the progressive, mild, dystrophic phenotype of A17 mice.

All mice appeared normal at birth and there was no difference in grip strength of the forelimbs or all limbs between non-transgenic, A17, BCL2 or A17 × BCL2 mice at 6 weeks of age (Fig. 1B and C). However, at 4 months of age, A17 mice were weaker than non-transgenic littermates as shown by grip strength of the forelimbs (Fig. 1B) and all limbs (Fig. 1C). A17 develop a progressive muscle weakness and had reduced grip strength compared with non-transgenic mice at 4 months of age, grip strength steadily declined until the end of the study (10 months of age). Muscle weakness was not seen in mice expressing both A17 and *BCL2* transgenes (A17 × BCL2 mice) at 4 months of age. BCL2 co-expression markedly improved grip strength in A17 mice, and A17 × BCL2 mice had a significantly increased forelimb and all-limb grip strength compared with A17 mice from 4 to 8 months of age (Fig. 1B and C). The beneficial effect of BCL2 co-expression on the grip strength of A17 mice was transient. A17 × BCL2 mice show a rapid decline in forelimb muscle strength from ∼6 months of age and all-limb muscle strength from ∼7 months of age and at 9 and 10 months of age, A17 × BCL2 had a similar forelimb grip strength and all-limb grip strength compared with A17 mice (Fig. 1B and C). The muscle weakness in A17 × BCL2 mice from ∼9 months of age is not due to the loss of expression of the BCL2 transgene; both A17 and *BCL2* transgenes are robustly expressed at 6 months and 11 months of age (Fig. 1A). The expression of BCL2 alone had no effect on grip strength in non-A17 mice, since BCL2 mice had a similar forelimb grip strength and all-limb grip strength to non-transgenic mice at all time points studied (Fig. 1B and C).

BCL2 co-expression also markedly improved the performance of A17 mice in accessory muscle strength tests (wire manoeuvre, vertical gripping, pelvic elevation) at early time points (Supplementary Material, Fig. S1). In many of these tests, A17 × BCL2 mice had a similar performance to non-transgenic mice at early time points. A17 × BCL2 mice performed significantly better than A17 mice at the wire manoeuvre task from 4 to 8 months of age and there was no significant difference in the performance of non-transgenic and A17 × BCL2 mice (Fig. 2A and Supplementary Material, Fig. S1). However, muscle weakness became apparent in A17 × BCL2 mice at later stages and there was no difference in performance at the wire manoeuvre task of A17 and A17 × BCL2 mice at 9 and 10 months of age. Fewer A17 × BCL2 mice dragged their pelvis when walking, compared with A17 mice at 8 and 9 months of age, but there was no significant difference in pelvic elevation between A17 and A17 × BCL2 mice at 10 months of age (Fig. 2B). A17 × BCL2 mice also had improved performance at the vertical gripping

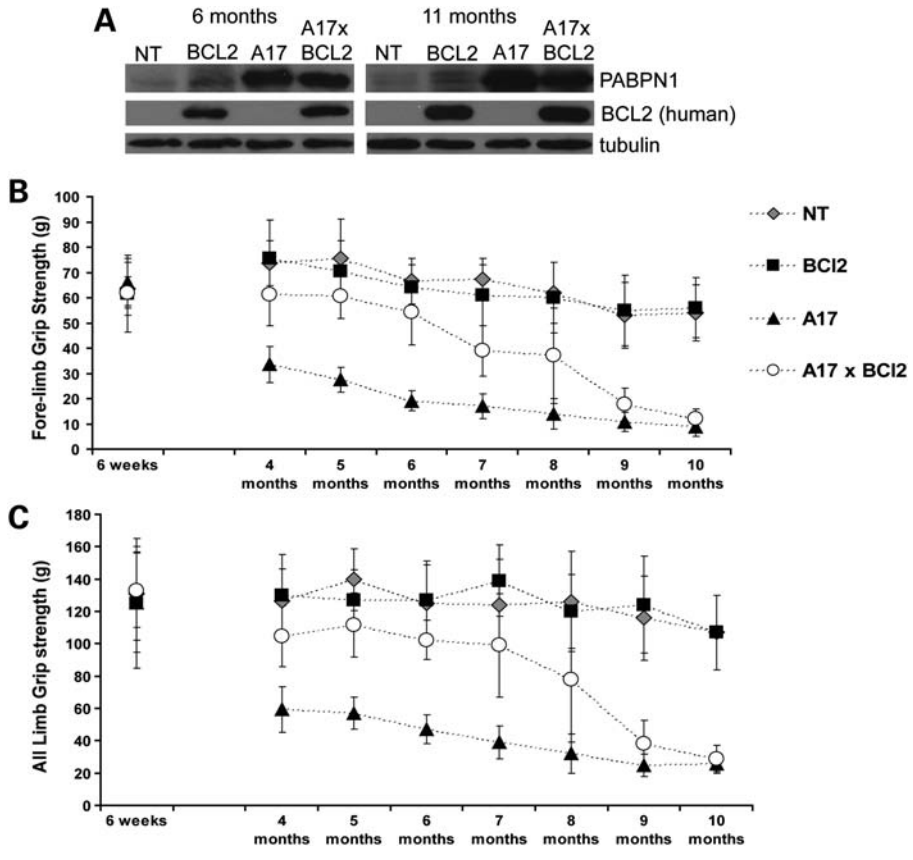

Figure 1. BCL2 expression improves grip strength at early time points in a mouse model of OPMD. (**A**) Western blot of biceps muscle lysates from 6 months and 11 months, A17 mice, non-transgenic mice (NT), BCL2 mice and A17 × BCL2 mice probed with antibodies against PABPN1 or human BCL2 (to show transgene levels). Tubulin was used as a loading control. (**B** and **C**) Forelimb grip strength (B) and grip strength of all limbs (C) of male A17 mice (black triangle; 6 weeks, $n = 17$; 4, 5 and 6 months, $n = 17$; 7 and 8 months, $n = 13$, 9 and 10 months, $n = 12$), non-transgenic mice (NT; grey diamond; 6 weeks, $n = 14$; 4, 5 and 6 months, $n = 14$; 7 and 8 months, $n = 11$; 9 and 10 months, $n = 10$), BCL2 mice (black square; 6 weeks, $n = 17$; 4, 5 and 6 months, $n = 17$; 7 and 8 months, $n = 13$; 9 and 10 months, $n = 12$) and mice expressing both A17 and BCL2 transgenes (A17 × BCL2; open circle; 6 weeks, $n = 17$; 4, 5 and 6 months, $n = 17$; 7, 8, 9 and 10 months, $n = 14$). (B) Forelimb grip strength was improved in A17 × BCL2 mice compared with A17 mice at 4 months ($P < 0.0001$), 5 months ($P < 0.0001$), 6 months ($P < 0.0001$), 7 months ($P < 0.0001$) and 8 months ($P = 0.0003$) of age but not at 9 months ($P = 0.08$) and 10 months ($P = 0.06$) of age. Repeated measure ANOVAs for determination of the overall effect from all time points P, <0.0001. (C) Grip strength from all limbs was improved in A17 × BCL2 mice compared with A17 mice at 4 months ($P < 0.0001$), 5 months ($P < 0.0001$), 6 months ($P < 0.0001$), 7 months ($P < 0.0001$) and 8 months ($P = 0.0006$) of age but not at 9 months ($P = 0.06$) and 10 months ($P = 0.3$) of age. Repeated measure ANOVAs for determination of the overall effect from all time points P, <0.0001. No significant difference in forelimb grip strength or grip strength from all limbs was seen between BCL2 mice and non-transgenic mice at all time points studied, or between any of the different groups at 6 weeks of age. Data were analysed using two-tailed Student's *t*-tests at each individual time point. Error bars represent SD.

task at early time points. More A17 × BCL2 mice were able to grip the vertical grid (rather than fall due to reduced muscle strength), compared with A17 mice at 7 and 8 months of age (Fig. 2C). However, there was no difference in performance at the vertical gripping task between A17 and A17 × BCL2 mice at 9 and 10 months of age (Fig. 2C). The expression of BCL2 alone had no effect on performance at any of these tasks and BCL2 mice performed the same as non-transgenic mice at all time points studied (Supplementary Material, Fig. S1). All groups performed similarly at 6 weeks of age (Fig. 2 and Supplementary Material, Fig. S1).

A17 mice have reduced weight compared with non-transgenic littermates and the mean weight of A17 mice is increased by the co-expression of BCL2

We observed that A17 mice had a reduced body weight compared with non-transgenic mice from the ages of 4–10 months (Fig. 3A). A17 × BCL2 mice had a significantly different distribution of body weights compared with A17 mice and had a higher average body weight than A17 mice from 4 to 10 months of age (Fig. 3A). The expression of BCL2 alone did not alter body weight, and BCL2 mice had similar body weights to non-transgenic mice at all time points studied. All groups had a similar weight distribution at 6 weeks of age (Fig. 3A).

Given the differences in body weight between non transgenic, A17 and A17 × BCL2 mice, we were interested in muscle mass of these mice. A17 mice had a reduced mass of the *tibialis anterior* (TA) and *quadriceps* muscle compared with non-transgenic mice at 6 months of age (Fig. 3B) and 11 months of age (Fig. 3C). The mass of the TA and *quadriceps* muscles was increased in A17 × BCL2 mice compared with A17 mice at 6 months of age (Fig. 3B) and at 11 months of age (Fig. 3C).

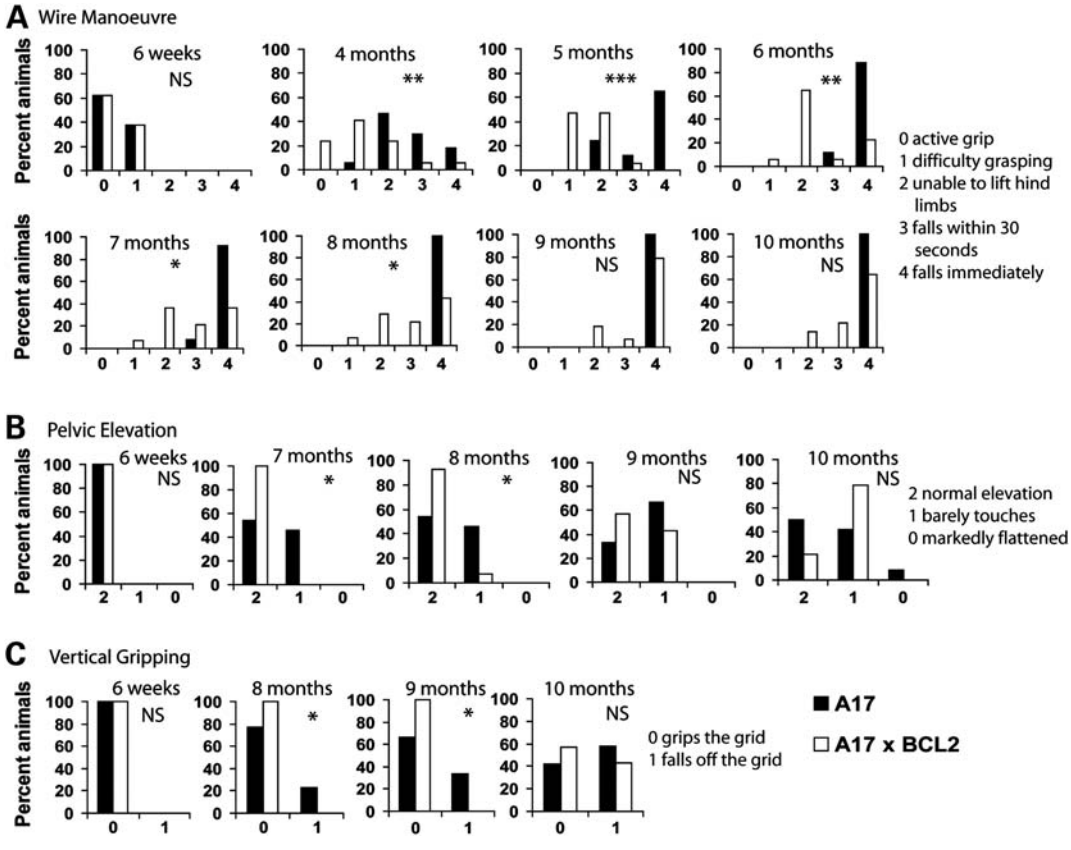

Figure 2. BCL2 expression transiently improves muscle strength in a mouse model of OPMD. Male A17 mice (black bar; 6 weeks, $n = 17$; 4, 5 and 6 months, $n = 17$; 7 and 8 months, $n = 13$; 9 and 10 months, $n = 12$) and male A17 × BCL2 mice (open bar; 6 weeks, $n = 17$; 4, 5 and 6 months, $n = 17$; 7, 8, 9 and 10 months, $n = 14$) were compared in strength tests. (**A**) A17 × BCL2 mice performed better than A17 mice at the wire manoeuvre task at 4, 5, 6, 7 and 8 months of age but not at 9 and 10 months of age. Score: 0, active grip with hind legs; 1, difficulty grasping with hind legs; 2, unable to lift hind legs; 3, falls within 30 s; 4, falls immediately. (**B**) Pelvic elevation was improved in A17 × BCL2 mice compared with A17 mice at the ages of 7 and 8 months but not at 9 and 10 months. Score: 2, normal elevation; 1, barely touches; 0, markedly flattened. (**C**) A17 × BCL2 males performed significantly better at the vertical gripping test at 8 and 9 months of age, but not at 10 months of age, compared with A17 males. Score: 0, grips the grid; 1, falls off the grid. $^{*}P < 0.05$; $^{**}P < 0.001$; $^{***}P < 0.0001$; NS, non-significant. Non-parametric data from the wire manoeuvre and pelvic elevation tests were analysed using Mann–Whitney *U*-tests and we used Chi-squared tests to analyse vertical gripping data.

BCL2 co-expression reduces apoptotic markers in A17 mice, even at late stages when BCL2 fails to rescue muscle weakness

We hypothesized that BCL2 co-expression would rescue muscle weakness by reducing levels of apoptosis in A17 mice. We were also interested to test levels of apoptosis at later stages in A17 mice, when BCL2 co- expression does not protect against muscle weakness. In accordance with previous data (12), we observed an increase in the number of TUNEL-positive nuclei in biceps muscle sections from A17 mice compared with non-transgenic mice at both 6 and 11 months of age (Fig. 4A). The number of TUNEL-positive nuclei was reduced in A17 × BCL2 mice compared with A17 mice at both 6 and 11 months of age (Fig. 4A). A17 × BCL2 mice have similar levels of TUNEL-positive nuclei to non-transgenic mice, even at 11 months of age when A17 × BCL2 mice manifest muscle weakness. Interestingly, the number of myofibre nuclei containing PABPN1-labelled aggregates was increased in muscle sections from A17 × BCL2 mice, compared with A17 mice at both 6 and 11 months of age (Fig. 4B and C). This phenomenon may be due to increased survival times of aggregate-containing myofibres due to BCL2.

Muscle sections from A17 mice showed an increase in the number of muscle fibres with a diffuse localization of cytochrome c (as opposed to mitochondrial localization, corresponding to cytochrome c release from the mitochondria) (Fig. 5A) and an increased number of muscle fibres positive for active caspase 3 (Fig. 5B) compared with sections from non-transgenic mice. These apoptotic markers were reduced in biceps muscle sections from A17 × BCL2 mice compared with A17 mice (Fig. 5A and B). The number of muscle fibres with a diffuse localization of cytochrome c (Fig. 5A) and number of muscle fibres positive for active caspase 3 (Fig. 5B) were decreased to non-transgenic levels in A17 × BCL2 mice, even at 11 months of age, suggesting that the muscle weakness seen at late stages in A17 × BCL2 mice is not due to excess apoptosis.

We also compared the histology of muscle sections from A17 and A17 × BCL2 mice and observed a decrease in the number of centralized nuclei (as a percentage of the total myoblast nuclei scored) in haematoxylin and eosin stained biceps sections from 6-month old A17 × BCL2 mice compared with

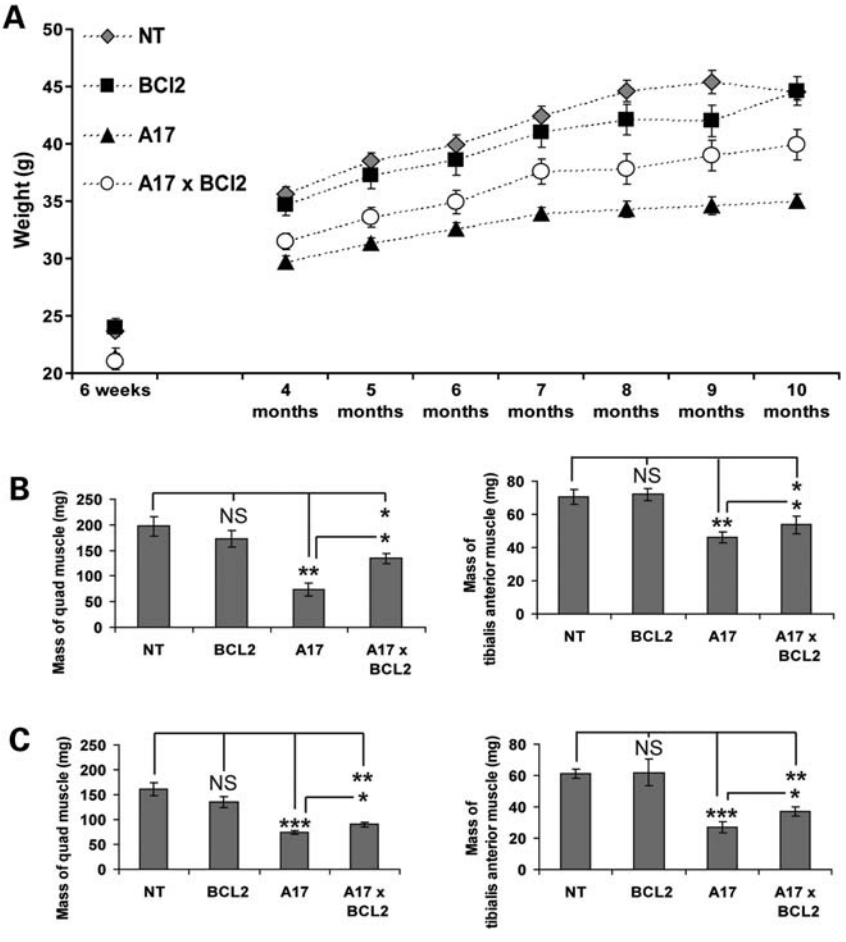

Figure 3. Weight differences between non-transgenic, A17, BCL2 and A17 × BCL2 mice. (**A**) Body weight of male A17 mice (black triangle; 6 weeks, $n = 17$; 4, 5 and 6 months, $n = 17$; 7 and 8 months, $n = 13$, 9 and 10 months, $n = 12$), non-transgenic mice (NT; grey diamond; 6 weeks, $n = 14$; 4, 5 and 6 months, $n = 14$; 7 and 8 months, $n = 11$; 9 and 10 months, $n = 10$), BCL2 mice (black square; 6 weeks, $n = 17$; 4, 5 and 6 months, $n = 17$; 7 and 8 months, $n = 13$; 9 and 10 months, $n = 12$) and mice expressing both A17 and BCL2 transgenes (A17 × BCL2; open circle; 6 weeks, $n = 17$; 4, 5 and 6 months, $n = 17$; 7, 8, 9 and 10 months, $n = 14$). Male A17 mice on a mixed FvB C57BL/6 background weighed less than non-transgenic littermates at 4 months ($P = 0.0001$), 5 months ($P < 0.0001$), 6 months ($P = 0.0004$), 7 months ($P = 0.004$), 8 months ($P = 0.0008$), 9 months ($P = 0.002$) and 10 months of age ($P = 0.002$). Repeated measure ANOVAs for determination of the overall effect from all time points P, <0.0001. Co-expression of BCL2 in A17 mice alters the distribution of body weights, and A17 × BCL2 mice generally weighed more than A17 mice at 4 months ($P = 0.04$), 5 months ($P = 0.02$), 6 months ($PP = 0.04$), 7 months ($P = 0.009$), 8 months ($P = 0.03$), 9 months ($P = 0.03$) and 10 months of age ($P = 0.008$) (repeated measure ANOVAs for determination of the overall effect from all time points P, <0.0001). The expression of BCL2 alone does not alter body weight, and there was no significant difference in body weight between BCL2 mice and NT mice at any time point studied. There was no difference in body weight between any of the groups at 6 weeks of age. (**B**) Muscle mass of *quadriceps* and *tibilias anterior* muscles from 6-month-old A17, NT, BCL2 and A17 × BCL2 mice ($n = 3$). (**C**) Muscle mass of *quadriceps* and *tibilias anterior* muscles from 11-month-old A17, NT, BCL2 and A17 × BCL2 mice ($n = 3$). $^{*}P < 0.05$; $^{**}P < 0.001$; $^{***}P < 0.0001$; NS, non-significant. Error bars represent SEM.

A17 mice (Fig. 5C). However, at 11 months of age, there was no difference in the percentage of centralized nuclei in muscle sections from A17 × BCL2 mice compared with A17 mice. After regeneration, muscle fibres are centrally nucleated. Centralized nuclei are thought to represent the degenerative/regenerative process occurring in muscle and are routinely used as a marker of dystrophic injury and subsequent regeneration (31,32).

DISCUSSION

Here we provide evidence that apoptosis is a major contributor to muscle weakness that is a characteristic feature of OPMD. Genetically blocking apoptosis by the over-expression of BCL2 ameliorates muscle weakness in A17 mice. Between 4 and 8 months of age, A17 × BCL2 mice perform better than A17 mice at grip strength, wire manoeuvre and vertical gripping tasks, and this is associated with a reduction in apoptotic markers in muscle sections. The co-expression of BCL2 in A17 mice has a large rescue effect on muscle weakness, with A17 × BCL2 mice performing similar to non-transgenic mice in many strength tests. This suggests an important role for excessive apoptosis in the pathogenesis of OPMD *in vivo,* at least early in the disease process.

We observed that A17 mice have reduced body weights compared with non-transgenic mice. This difference has not been so apparent in our previous studies when the A17

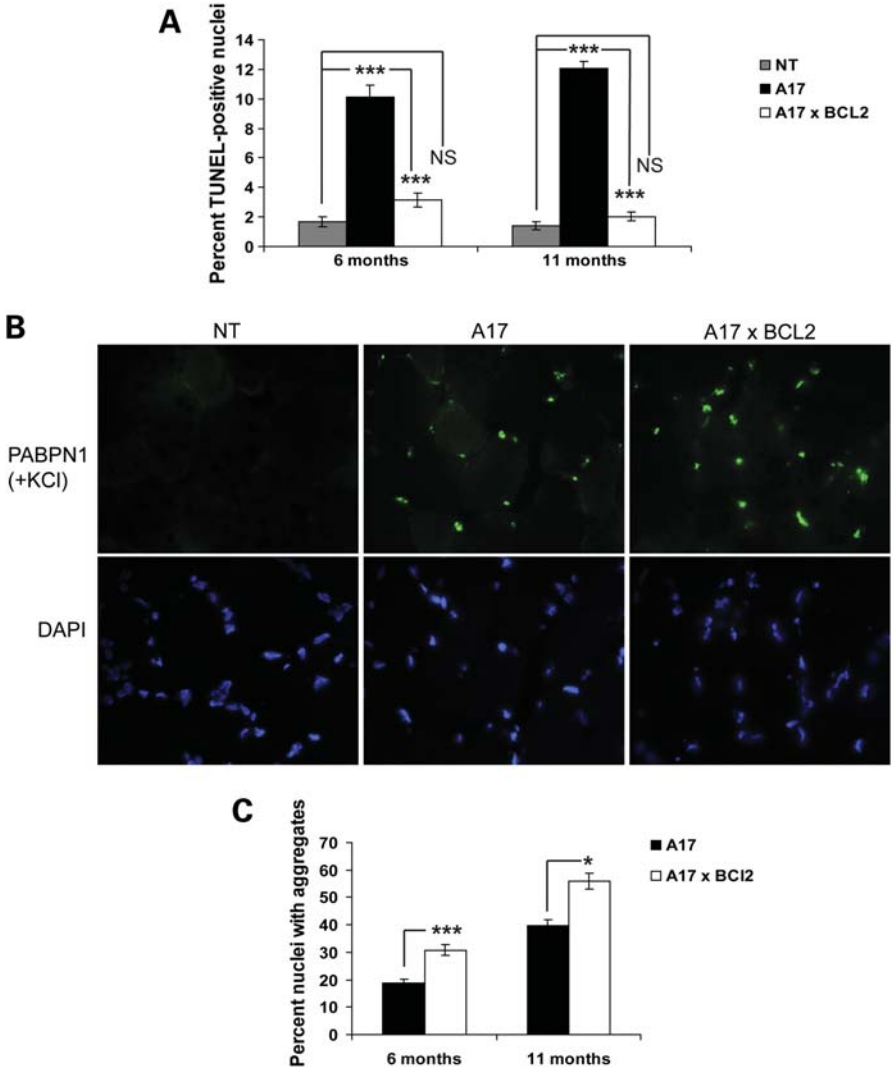

Figure 4. Cell death and aggregate load in A17 mice and mice expressing both A17 and BCL2 transgenes. (**A**) Biceps muscle sections from 6-month-old and 11-month-old A17 (black bar), NT (grey bar) and A17 × BCL2 (open bar) mice were TUNEL labelled and the number of positive nuclei scored. (**B**) Representative images of PABPN1-labelled aggregates (green) in biceps muscle sections from 6-month-old A17 mice and A17 × BCL2 mice. Sections were treated with KCl prior to labelling to remove soluble proteins (aggregates are resistant) and hence no signal is seen in sections from non-transgenic (NT) mice. Nuclei were visualized using DAPI (blue). (**C**) Quantification of the number of nuclei containing PABPN1-labelled aggregates in sections from 6-month-old and 11-month-old A17 mice (black bar) and A17 × BCL2 (open bar) mice treated as (B). $n = 3$; $^{*}P < 0.05$; $^{***}P < 0.0001$. Error bars represent SEM.

transgene was on the FvB background (12,15). The larger difference in body weight between A17 and non-transgenic mice seen in this study may be due to the A17 transgene being expressed on a mixed FvB C57BL/6 background. A17 × BCL2 mice have a higher average body weight than A17 mice. We also show differences in muscle mass. TA and *quadriceps* muscle mass are reduced in A17 mice compared with non-transgenic mice. This reduction in muscle mass is likely to be due to muscle atrophy that has been demonstrated in A17 mice (33). Co-expression of BCL2 in A17 mice reduces atrophy and the mass of TA and *quadriceps* muscles is increased in A17 × BCL2 mice compared with A17 mice. Interestingly, a recent study has suggested that muscle wasting and atrophy in myotonic dystrophy primarily results from activation of apoptosis (34).

The dramatic improvement in muscle strength of A17 mice due to BCL2 co-expression is transient, and BCL2 overexpression afforded protection against muscle weakness at 8, 9 and 10 months of age. This muscle weakness occurred despite a marked reduction in apoptotic markers like TUNEL-positive nuclei, myofibres labelled for active-caspase 3 and myofibres showing a diffuse localization of cytochrome c, in the A17 × BCL2 mice at 11 months of age. Indeed, at 11 months of age, muscle sections from A17 × BCL2 mice had levels of apoptotic markers similar to non-transgenic mice. This suggests that other cell death pathways may be activated in A17 × BCL2 mice from ∼8 months of age, or that the A17 insult eventually causes muscle weakness via mechanisms distinct from cell death. While apoptosis is unlikely to be the exclusive pathway of myofibre death in A17 muscle, our data suggest that apoptosis is the major pathway.

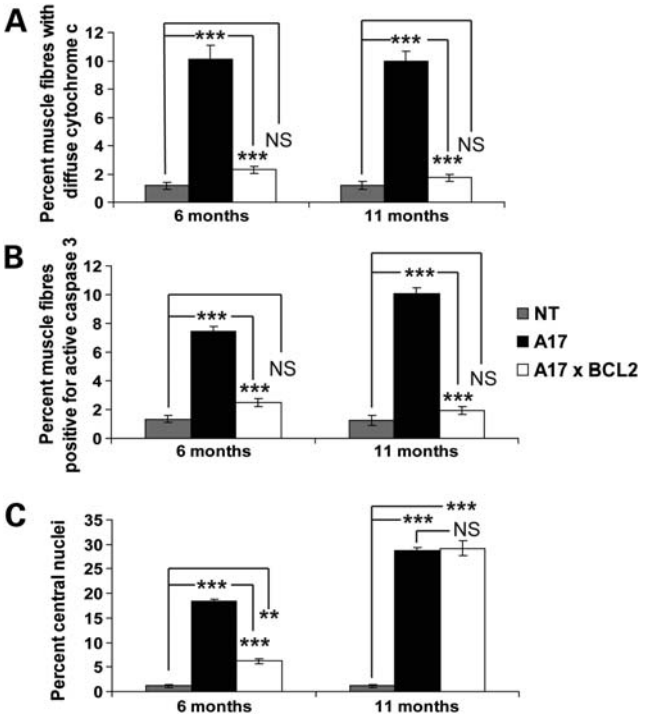

Figure 5. Apoptotic markers are elevated in muscle from A17 mice and reduced by BCL2 co-expression. (**A**) Quantification of the number of myofibres with a diffuse pattern of cytochrome c labelling (corresponding to cytochrome c release from the mitochondria to cytosol and indicating apoptotic myofibres) in biceps muscle sections from 6-month-old and 12-month-old NT, A17 and A17 × BCL2 mice. (**B**) Biceps muscle sections from 6-month-old and 12-month-old NT, A17 and A17 × BCL2 mice were labelled with an active caspase 3 antibody and the number of immuno-positive myofibres were scored. (**C**) Quantification of the number of centralized nuclei in H&E stained biceps sections from 6-month-old and 12-month-old NT, A17 and A17 × BCL2 mice. Apoptotic markers are reduced in A17 × BCL2 mice to NT levels even at 11 months when BCL2 does not rescue phenotype and muscle weakness is apparent in A17 × BCL2 mice ($n = 3$). $^{**}P < 0.001$; $^{***}P < 0.0001$; NS, non-significant. Error bars represent SEM.

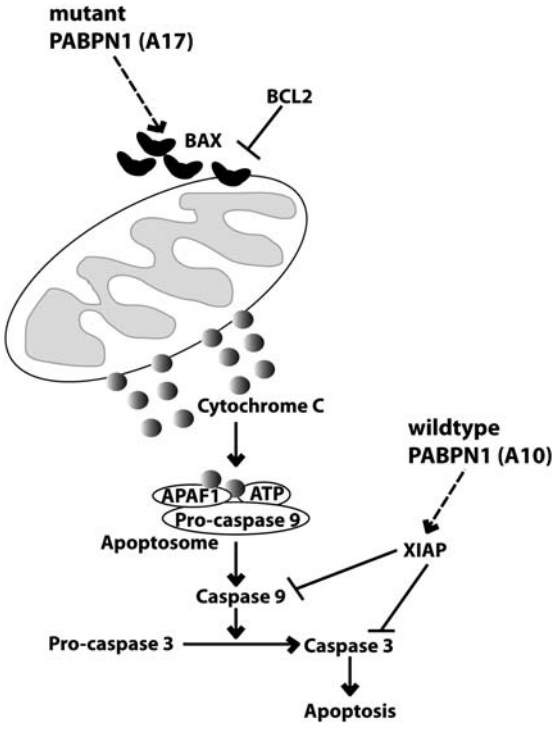

Figure 6. A central role for apoptosis in the pathogenesis of OPMD. The expression of mutant PABPN1 (A17) results in increased levels of BAX (12). This causes the activation of the apoptotic cascade (12,15). Cytochrome c is released from the mitochondria to the cytosol where it can bind additional factors to form the apoptosome complex. The apoptosome complex causes the conversion of procaspases to their active, mature caspase form and ultimately results in the activation of caspase 3, otherwise known as the executioner caspase. Here we have provided data to further support a central role of apoptosis in the pathogenesis of OPMD. Genetically blocking apoptosis by the over-expression of BCL2 ameliorates A17 toxicity. BCL2 most likely acts to block A17 toxicity by binding the excess BAX and sequestering it away from the mitochondria. Wild-type PABPN1 has an opposing effect on apoptosis and increases the translation of XIAP, a caspase inhibitor (38). It is likely that OPMD is primarily caused by a toxic gain of function of mutant PABPN1 that results in the activation of apoptosis. However, the loss of the anti-apoptotic function of wild-type PABPN1 may also contribute to pathology.

It is unlikely that apoptosis is a pathway that is specific to OPMD and it may be involved in the pathogenesis of other muscular dystrophies. Apoptotic markers have been observed in biopsy samples from some muscular dystrophy patients (35) and in mouse models of muscular dystrophy (27,36). Apoptosis and the activation of apoptotic pathways are evident in mouse models of myopathy including collagen VI-deficient mice (22), caveolin-3 mutant mice that model limb girdle muscular dystrophy (24) and calpain 3-deficient mice that model limb girdle muscular dystrophy type 2A (20). Anti-apoptotic strategies, such as blocking the mitochondrial permeability transition pore by treatment with cyclosporine A, have been shown to rescue mouse models of collagen VI deficiency (22) and correct mitochondrial dysfunction and muscle apoptosis in patients with collagen VI myopathies (19). In addition, blocking apoptosis by the over-expression of BCL2 ameliorates muscle disease in a laminin α-2-deficient mouse model of congenital muscular dystrophy (17,18). However, BCL2 over-expression failed to attenuate the disease phenotype of the mdx mouse (18). Thus, in Duchenne and certain other muscular dystrophies, it is possible that other cell death pathways such as necrosis may be more important mediators of pathology, and death of myofibres may result from the interplay of various pathways.

While we propose that apoptosis is central to OPMD, the therapeutic value of blocking apoptosis using BCL2 induction in muscle may be limited by its tractability. However, the BCL2 experiment provides further mechanistic support for the consideration of drugs such as doxycycline, trehalose and cystamine which attenuate the disease phenotype of our mouse model of OPMD. Doxycycline (12), trehalose (16) and cystamine (15) act, in part, by inhibiting apoptosis but also have effects upstream of the induction of apoptosis such as reducing the aggregation of mutant PABPN1 (doxycycline, trehalose and cystamine), decreasing transglutaminase 2 activity (cystamine) and reducing levels of mutant PABPN1 (trehalose). Doxycycline has also been used to alleviate the disease phenotype of the laminin α-2-deficient mouse and this is thought to occur via its inhibitory action on apoptosis (37). While the almost complete block of apoptosis by the

over-expression of BCL2 had a profound rescue effect on muscle weakness and pathology in the OPMD mouse at early time points, the BCL2 overexpression was not beneficial at later time points. It is likely that when apoptosis is blocked, there is an activation of alternative cell death pathways that cause the termination of a dysfunctional muscle fibre that is already committed to die. Apoptosis is central to OPMD but is a downstream event in pathology. It may be more beneficial to additionally target events that are upstream of apoptosis in OPMD pathogenesis, such as the aggregation of mutant PABPN1 and the levels (degradation) of mutant PABPN1.

Theoretically, the long-term upregulation of BCL2 and the subsequent blocking of apoptosis could have adverse effects in the mouse such as tumourogenesis. However, mice over-expressing BCL2 specifically in muscle (MRF4-hBCL2 mice) do not develop a phenotype (17,18) and in this study were indistinguishable from non-transgenic mice up to 11 months of age (when sacrificed in this study).

We now propose a model where apoptosis is central to OPMD (Fig. 6). We have previously shown that the expression of mutant PABPN1 (A17) results in increased levels of BAX and the upregulation of apoptotic markers (12,15). While the expression of mutant PABPN1 induces cell death, wild-type PABPN1 is protective and can reduce toxicity caused by pro-apoptotic agents and mutant PABPN1 expression via the translational regulation of X-linked inhibitor of apoptosis (XIAP) (38). It is possible that there is a loss-of-function element to OPMD, as the increase in protein levels of XIAP in skeletal muscle of A10 mice was not seen in muscle from A17 mice (38). Here we have shown that genetically blocking apoptosis by the over-expression of BCL2 ameliorates A17 toxicity. BCL2 most likely acts to block A17 toxicity by binding the excess BAX and sequestering it away from the mitochondria. We have previously used apoptosis as a marker for the toxicity of mutant PABPN1 in our cell and mouse models of OPMD. However, it is likely that the apoptotic pathway is major contributor to muscle weakness and dysfunction in OPMD.

MATERIALS AND METHODS

Transgenic mice

All studies and procedures were carried out following UK Home Office regulations and animals were caged under standard conditions (12 h light, 12 h dark; food and water available *ad libitum*). OPMD transgenic mice [A17-1 mice (12)] express a mutant, expanded *PABPN1* transgene under control of the human skeletal actin (*HSA*) promoter on the FvB background (12). Mice expressing human BCL2 under control of the myogenin regulatory factor 4 (MRF4) promoter (MRF4-hBCL2 mice) were obtained from J Boone Miller and J Dominov, Boston Biomedical Research Institute, and are on the C57BL/6 background (17). Mice heterozygous for the A17 transgene were crossed with mice heterozygous for the human *BCL2* transgene to produce F1 litters comprising non-transgenic mice, mice expressing the A17 transgene (A17 mice), mice expressing the h*BCL2* transgene (BCL2 mice) and mice expressing both the A17 and h*BCL2* transgene (A17 × BCL2 mice) on a mixed F1 FvB C57BL/6 background.

Genotyping

Genotype was determined using PCR. Genomic DNA was isolated from ear biopsies by lysis in 0.25 mg/ml proteinase K in 1% SDS, 100 mM NaCl, 100 mM EDTA, 50 mM Tris, pH 8 at 55°C for 1 h in the presence of 10% (w/v) chelex (Bio Rad Laboratories). Proteinase K was inactivated by incubating the sample at 95°C for 15 min. Chelex was precipitated by centrifugation and the supernatant, containing genomic DNA, was used for PCR. We determined the presence of the *PABPN1* transgene using the primers 5′-GAACCAACAGACCAGGCATC-3′ and 5′-AGGACTGACACGTGCTACGA-3′. The h*BCL2* transgene was detected using the primers 5′-TAGATGTTCTGGGG AGCACTAGC-3′ and 5′-CACTCGTAGCCCCTCTGCGA CAG-3′. The PCR mix contained ∼20–100 ng genomic DNA, 200 μM dNTPs, 100 nM each primer, 2 units Taq DNA polymerase I (5 units/μl; Promega) in 1 × buffer (50 mM KCl, 10 mM Tris-Cl, pH 9.0, 0.1% Triton® X-100; Promega) supplemented with 1.5 mM $MgCl_2$ and 5% DMSO. Fragments were amplified under the following PCR conditions: 94°C for 1 min; 60°C for 2 min, 72°C for 1 min for 30 cycles; then 72°C for 10 min.

Strength testing of mice

F1, male non-transgenic, A17, BCL2 and A17 × BCL2 mice were tested at 6 weeks of age, then monthly from 4 months of age. Mice were given alphanumeric identities that provided no clue to genotype. Grip strength of the forelimbs and all limbs was assessed using a grip strength metre (Bioseb). Wire manoeuvre, pelvic elevation and vertical gripping are part of the SHIRPA battery of behavioural tests (39). For the wire manoeuvre, we held mice above a horizontal wire by the tail and lowered them to allow the forelimbs to grip the wire. Mice were held in extension, rotated around to the horizontal and released. Mice were scored as follows: 0, active grip with hind legs; 1, difficulty grasping with hind legs; 2, unable to lift hind legs; 3, falls within 30 s; 4, falls immediately. For the vertical gripping test, we placed mice on a horizontal grid that was gripped with both forelimbs and hind limbs. We raised the grid to the vertical and scored mice as follows: 0, grips the grid; 1, falls off the grid. We also assessed mice for elevation of the pelvis when walking and scored them as follows: 0, markedly flattened; 1, barely touches; 2, normal (3 mm elevation). We analysed non-parametric data from the wire manoeuvre and pelvic elevation tests at each time point using Mann–Whitney *U*-tests (STATVIEW software, version 4.53; Abacus Concepts). We used Chi-squared tests to analyse vertical gripping data. We analysed grip strength meter data from each treatment time point with unpaired *t*-tests and the overall effect from all treatment time points with repeated-measures ANOVA (STATVIEW software, version 4.53; Abacus Concepts).

Western blotting

Lysates were prepared by homogenizing tissue in 50 mM Tris–HCl pH 7.4, 0.5% Triton X-100 with protease inhibitor cocktail (Complete; Roche Diagnostics). Proteins were separated on 10% SDS–polyacrylamide gels and transferred onto

nitrocellulose membranes (Hybond ECL membrane; Amersham Biosciences), which were blocked by incubation in 5% dried milk in 0.1 M PBS, 0.1% Tween-20, pH 7.6. Membranes were probed with primary antibodies raised against PABPN1 (1:10,000), human BCL2 (Cell Signalling Technologies; 1:1000) or as loading control tubulin (Sigma Aldrich; 1:1000). HRP-conjugated antibodies (Amersham Biosciences; 1:5000) were then added to the blots. Immuno-reactive bands were detected with enhanced chemiluminescence reagent (ECL; Amersham Biosciences) and signal visualized by the exposing membrane to ECL Hyperfilm (Amersham Biosciences).

Histology

Tissue was snap frozen in liquid nitrogen-cooled isopentane and 10 μm sections were cut on a cryostat (Leica Microsystems) to poly-L-lysine-coated slides. Sections were fixed in acetone. For immuno-labelling, slides were blocked with 1% normal goat serum in 0.1 M PBS, 0.1% Triton X-100 and then incubated, at 4°C overnight, in primary antibody diluted in 1% normal goat serum in 0.1 M PBS, 0.1% Triton X-100. Primary antibodies used were anti-PABPN1 (1:1000), cytochrome c (Pharmingen; 1:500) or active caspase 3 (Promega; 1:250). Slides were washed in 0.1 M PBS, 0.1% Triton X-100 and incubated in fluorophore-conjugated secondary antibody (Alexa Fluor 488 goat anti-rabbit or Alexa Fluor 594 goat anti-mouse; 1:1000; Molecular Probes) for 2 h at room temperature in the dark. Slides were washed again and sections mounted in citifluor (Citifluor Ltd.) containing 4′,6-diamidino-2-phenylindole (DAPI; 3 μg/ml; Sigma-Aldrich Ltd.) to visualize nuclei. To remove soluble proteins, sections were incubated in 1 M KCl, 30 mM HEPES, 65 mM PIPES, 10 mM EDTA, 2 mM $MgCl_2$, pH 6.9 for 1 h at room temperature prior to immuno-labelling. Aggregates are resistant to this KCl treatment. As negative controls to check for non-specific fluorescence, sections were processed as above but with either primary or secondary antibody omitted. For histological analysis of muscle morphology and pathology, sections were stained with haemotoxylin and eosin (H&E). Fluorescent DNA fragmentation (TUNEL; terminal deoxynucleotidyl transferase-mediated dUTP nick end labelling) assay was carried out on skeletal muscle sections using a standard kit (ApoAlert DNA fragmentation assay kit; BD Biosciences).

Nuclei that contained aggregates, TUNEL-positive nuclei, centralized nuclei, myofibres immunoreactive for active caspase 3 and myofibres with a diffuse, cytosolic pattern of cytochrome c labelling were scored. Three samples per group and 200 nuclei per sample were scored with the viewer blind to the identity of the slide. Pooled estimates were calculated as odds ratios [OR; the ratios of the proportion of aggregate containing/normal (or TUNEL positive/TUNEL negative) nuclei in different experimental conditions] with 95% confidence intervals, as described previously. OR and *P*-values were determined by unconditional logistical regression analysis using the general log linear analysis option of SPSS Version 6.1. Images were taken with a LSM510 confocal microscope (Leica).

SUPPLEMENTARY MATERIAL

Supplementary Material is available at *HMG* online.

ACKNOWLEDGEMENTS

We thank O. Sadiq and F. Siddiqi for technical assistance, and S. Luo and M. Garcia Arencibia for helpful comments on the manuscript. We are grateful to J. Dominov and J. Boone Miller for the MRF4-hBCL2 mice.

Conflict of Interest statement. None declared.

FUNDING

This work was funded by the Wellcome Trust (Senior Fellowship to D.C.R.). Funding to pay the Open Access publciation charges for this article was provided by the Wellcome Trust.

REFERENCES

1. Abu-Baker, A. and Rouleau, G.A. (2007) Oculopharyngeal muscular dystrophy: recent advances in the understanding of the molecular pathogenic mechanisms and treatment strategies. *Biochim. Biophys. Acta*, **1772**, 173–185.
2. Davies, J.E., Berger, Z. and Rubinsztein, D.C. (2006) Oculopharyngeal muscular dystrophy: potential therapies for an aggregate-associated disorder. *Int. J. Biochem. Cell Biol.*, **38**, 1457–1462.
3. Schmitt, H.P. and Krause, K.H. (1981) An autopsy study of a familial oculopharyngeal muscular dystrophy (OPMD) with distal spread and neurogenic involvement. *Muscle Nerve*, **4**, 296–305.
4. van der Sluijs, B.M., van Engelen, B.G. and Hoefsloot, L.H. (2003) Oculopharyngeal muscular dystrophy (OPMD) due to a small duplication in the PABPN1 gene. *Hum. Mutat.*, **21**, 553.
5. Blumen, S.C., Brais, B., Korczyn, A.D., Medinsky, S., Chapman, J., Asherov, A., Nisipeanu, P., Codere, F., Bouchard, J.P., Fardeau, M. *et al.* (1999) Homozygotes for oculopharyngeal muscular dystrophy have a severe form of the disease. *Ann. Neurol.*, **46**, 115–118.
6. Brais, B., Bouchard, J.P., Xie, Y.G., Rochefort, D.L., Chretien, N., Tome, F.M., Lafreniere, R.G., Rommens, J.M., Uyama, E., Nohira, O. *et al.* (1998) Short GCG expansions in the PABP2 gene cause oculopharyngeal muscular dystrophy. *Nat. Genet.*, **18**, 164–167.
7. Tome, F.M. and Fardeau, M. (1980) Nuclear inclusions in oculopharyngeal dystrophy. *Acta Neuropathol.*, **49**, 85–87.
8. Uyama, E., Tsukahara, T., Goto, K., Kurano, Y., Ogawa, M., Kim, Y.J., Uchino, M. and Arahata, K. (2000) Nuclear accumulation of expanded PABP2 gene product in oculopharyngeal muscular dystrophy. *Muscle Nerve*, **23**, 1549–1554.
9. Bao, Y.P., Cook, L.J., O'Donovan, D., Uyama, E. and Rubinsztein, D.C. (2002) Mammalian, yeast, bacterial, and chemical chaperones reduce aggregate formation and death in a cell model of oculopharyngeal muscular dystrophy. *J. Biol. Chem.*, **277**, 12263–12269.
10. Abu-Baker, A., Messaed, C., Laganiere, J., Gaspar, C., Brais, B. and Rouleau, G.A. (2003) Involvement of the ubiquitin-proteasome pathway and molecular chaperones in oculopharyngeal muscular dystrophy. *Hum. Mol. Genet.*, **12**, 2609–2623.
11. Fan, X., Dion, P., Laganiere, J., Brais, B. and Rouleau, G.A. (2001) Oligomerization of polyalanine expanded PABPN1 facilitates nuclear protein aggregation that is associated with cell death. *Hum. Mol. Genet.*, **10**, 2341–2351.
12. Davies, J.E., Wang, L., Garcia-Oroz, L., Cook, L.J., Vacher, C., O'Donovan, D.G. and Rubinsztein, D.C. (2005) Doxycycline attenuates and delays toxicity of the oculopharyngeal muscular dystrophy mutation in transgenic mice. *Nat. Med.*, **11**, 672–677.
13. Hino, H., Araki, K., Uyama, E., Takeya, M., Araki, M., Yoshinobu, K., Miike, K., Kawazoe, Y., Maeda, Y., Uchino, M. *et al.* (2004) Myopathy phenotype in transgenic mice expressing mutated PABPN1 as a model of oculopharyngeal muscular dystrophy. *Hum. Mol. Genet.*, **13**, 181–190.

14. Chartier, A., Benoit, B. and Simonelig, M. (2006) A Drosophila model of oculopharyngeal muscular dystrophy reveals intrinsic toxicity of PABPN1. *EMBO J.*, **25**, 2253–2262.
15. Davies, J.E., Rose, C., Sarkar, S. and Rubinsztein, D.C. (2010) Cystamine suppresses polyalanine toxicity in a mouse model of oculopharyngeal muscular dystrophy. *Sci. Transl. Med.*, **2**, 34ra40.
16. Davies, J.E., Sarkar, S. and Rubinsztein, D.C. (2006) Trehalose reduces aggregate formation and delays pathology in a transgenic mouse model of oculopharyngeal muscular dystrophy. *Hum. Mol. Genet.*, **15**, 23–31.
17. Dominov, J.A., Kravetz, A.J., Ardelt, M., Kostek, C.A., Beermann, M.L. and Miller, J.B. (2005) Muscle-specific BCL2 expression ameliorates muscle disease in laminin α-2-deficient, but not in dystrophin-deficient, mice. *Hum. Mol. Genet.*, **14**, 1029–1040.
18. Girgenrath, M., Dominov, J.A., Kostek, C.A. and Miller, J.B. (2004) Inhibition of apoptosis improves outcome in a model of congenital muscular dystrophy. *J. Clin. Invest.*, **114**, 1635–1639.
19. Merlini, L., Angelin, A., Tiepolo, T., Braghetta, P., Sabatelli, P., Zamparelli, A., Ferlini, A., Maraldi, N.M., Bonaldo, P. and Bernardi, P. (2008) Cyclosporin A corrects mitochondrial dysfunction and muscle apoptosis in patients with collagen VI myopathies. *Proc. Natl Acad. Sci. USA*, **105**, 5225–5229.
20. Baghdiguian, S., Martin, M., Richard, I., Pons, F., Astier, C., Bourg, N., Hay, R.T., Chemaly, R., Halaby, G., Loiselet, J. *et al.* (1999) Calpain 3 deficiency is associated with myonuclear apoptosis and profound perturbation of the IkappaB alpha/NF-kappaB pathway in limb-girdle muscular dystrophy type 2A. *Nat. Med.*, **5**, 503–511.
21. Mukasa, T., Momoi, T. and Momoi, M.Y. (1999) Activation of caspase-3 apoptotic pathways in skeletal muscle fibers in laminin α-2-deficient mice. *Biochem. Biophys. Res. Commun.*, **260**, 139–142.
22. Irwin, W.A., Bergamin, N., Sabatelli, P., Reggiani, C., Megighian, A., Merlini, L., Braghetta, P., Columbaro, M., Volpin, D., Bressan, G.M. *et al.* (2003) Mitochondrial dysfunction and apoptosis in myopathic mice with collagen VI deficiency. *Nat. Genet.*, **35**, 367–371.
23. Basset, O., Boittin, F.X., Cognard, C., Constantin, B. and Ruegg, U.T. (2006) Bcl-2 overexpression prevents calcium overload and subsequent apoptosis in dystrophic myotubes. *Biochem. J.*, **395**, 267–276.
24. Smythe, G.M., Eby, J.C., Disatnik, M.H. and Rando, T.A. (2003) A caveolin-3 mutant that causes limb girdle muscular dystrophy type 1C disrupts Src localization and activity and induces apoptosis in skeletal myotubes. *J. Cell Sci.*, **116**, 4739–4749.
25. Benayoun, B., Baghdiguian, S., Lajmanovich, A., Bartoli, M., Daniele, N., Gicquel, E., Bourg, N., Raynaud, F., Pasquier, M.A., Suel, L. *et al.* (2008) NF-kappaB-dependent expression of the antiapoptotic factor c-FLIP is regulated by calpain 3, the protein involved in limb-girdle muscular dystrophy type 2A. *FASEB J.*, **22**, 1521–1529.
26. Sandri, M., Massimino, M.L., Cantini, M., Giurisato, E., Sandri, C., Arslan, P. and Carraro, U. (1998) Dystrophin deficient myotubes undergo apoptosis in mouse primary muscle cell culture after DNA damage. *Neurosci. Lett.*, **252**, 123–126.
27. Honda, A., Abe, S., Hiroki, E., Honda, H., Iwanuma, O., Yanagisawa, N. and Ide, Y. (2007) Activation of caspase 3, 9, 12, and Bax in masseter muscle of mdx mice during necrosis. *J. Muscle Res. Cell Motil.*, **28**, 243–247.
28. Migheli, A., Mongini, T., Doriguzzi, C., Chiado-Piat, L., Piva, R., Ugo, I. and Palmucci, L. (1997) Muscle apoptosis in humans occurs in normal and denervated muscle, but not in myotonic dystrophy, dystrophinopathies or inflammatory disease. *Neurogenetics*, **1**, 81–87.
29. Hua, C., Zorn, S., Jensen, J.P., Coupland, R.W., Ko, H.S., Wright, J.J. and Bakhshi, A. (1988) Consequences of the t(14;18) chromosomal translocation in follicular lymphoma: deregulated expression of a chimeric and mutated BCL-2 gene. *Oncogene Res.*, **2**, 263–275.
30. Hotchkiss, R.S., Strasser, A., McDunn, J.E. and Swanson, P.E. (2009) Cell death. *N. Engl. J. Med.*, **361**, 1570–1583.
31. Ontell, M., Feng, K.C., Klueber, K., Dunn, R.F. and Taylor, F. (1984) Myosatellite cells, growth, and regeneration in murine dystrophic muscle: a quantitative study. *Anat. Rec.*, **208**, 159–174.
32. Harris, J.B. and Johnson, M.A. (1978) Further observations on the pathological responses of rat skeletal muscle to toxins isolated from the venom of the Australian tiger snake, Notechis scutatus scutatus. *Clin. Exp. Pharmacol. Physiol.*, **5**, 587–600.
33. Trollet, C., Anvar, S.Y., Venema, A., Hargreaves, I.P., Foster, K., Vignaud, A., Ferry, A., Negroni, E., Hourde, C., Baraibar, M.A. *et al.* (2010) Molecular and phenotypic characterization of a mouse model of oculopharyngeal muscular dystrophy reveals severe muscular atrophy restricted to fast glycolytic fibres. *Hum. Mol. Genet.*, **19**, 2191–2207.
34. Loro, E., Rinaldi, F., Malena, A., Masiero, E., Novelli, G., Angelini, C., Romeo, V., Sandri, M., Botta, A. and Vergani, L. (2010) Normal myogenesis and increased apoptosis in myotonic dystrophy type-1 muscle cells. *Cell Death Differ.*, **17**, 1315–1324.
35. Tews, D.S. and Goebel, H.H. (1997) DNA-fragmentation and expression of apoptosis-related proteins in muscular dystrophies. *Neuropathol. Appl. Neurobiol.*, **23**, 331–338.
36. Tidball, J.G., Albrecht, D.E., Lokensgard, B.E. and Spencer, M.J. (1995) Apoptosis precedes necrosis of dystrophin-deficient muscle. *J. Cell Sci.*, **108**, 2197–2204.
37. Girgenrath, M., Beermann, M.L., Vishnudas, V.K., Homma, S. and Miller, J.B. (2009) Pathology is alleviated by doxycycline in a laminin-α-2-null model of congenital muscular dystrophy. *Ann. Neurol.*, **65**, 47–56.
38. Davies, J.E., Sarkar, S. and Rubinsztein, D.C. (2008) Wild-type PABPN1 is anti-apoptotic and reduces toxicity of the oculopharyngeal muscular dystrophy mutation. *Hum. Mol. Genet.*, **17**, 1097–1108.
39. Rogers, D.C., Fisher, E.M., Brown, S.D., Peters, J., Hunter, A.J. and Martin, J.E. (1997) Behavioral and functional analysis of mouse phenotype: SHIRPA, a proposed protocol for comprehensive phenotype assessment. *Mamm. Genome*, **8**, 711–713.